ELSEVIER

Journal of Power Sources 62 (1996) 179–186

JOURNAL OF POWER SOURCES

# Electrochemical intercalation of lithium into different varieties of carbon in solid polymer electrolyte

F. Coowar [a], D. Billaud [a,*], J. Ghanbaja [a], P. Baudry [b]

[a] *Laboratoire de Chimie Minérale Appliquée, URA CNRS 158, Université de Nancy I, BP 239, 54506 Vandoeuvre-lès-Nancy Cedex, France*

[b] *EDF–DER, Les Renardières, Route de Sens, BP 1, Ecuelles, 77250 Moret-sur-Loing, France*

Received 2 February 1996; revised 29 March 1996; accepted 24 April 1996

**Abstract**

The electrochemical intercalation of lithium into different varieties of carbon was carried out using a solid polymer electrolyte. The faradaic efficiency obtained in the first cycle is relatively low compared with those obtained with a liquid electrolyte. The specific capacity exhibited by graphite materials is greater than that displayed with coke. A discharge capacity of 290 mAh/g after 15 cycles is encountered with a synthetic graphite, for which the variation in impedance before and after cycling was less significant. For natural graphite, a decrease in discharge capacity was found to be associated with an increase in impedance. This probably involves an irreversible reduction of the electrolyte which is more likely to occur on natural graphite presenting a greater BET surface area. Analysis by electron energy loss spectroscopy shows that the graphite surface was covered with carbonates.

*Keywords:* Lithium intercalation; Carbonaceous materials; Solid polymer electrolytes

## 1. Introduction

Lithium batteries operating with a liquid electrolyte have reached the market only in 1990 [1]. The major bottleneck to this late development is linked to the high reactivity of lithium, the growth of lithium dendrites which can short-circuit the cells, and to the safety issues. Moreover, the morphology of the plated lithium on the lithium anode has a substantial effect on cycling. The dendrites deposited during cycling on the anode give rise to small inactive particles of lithium of high specific area which reduce drastically the cycle life of the battery.

Such a problem may be overcome by the use of an alloy of β-Li–Al [2,3]. This material reduces the dendrite formation and, therefore, an extended cycle life can be achieved. However, during the addition and removal of lithium into this material, the volume of the latter, due to the phase transformation that occurs, is altered significantly and will lead to mechanical instability [4].

Another alternative to this problem consists in selecting materials displaying the following properties: high specific capacity, low potential with respect to lithium and stable and compatible with a great variety of electrolyte.

These properties are fulfilled by carbonaceous materials which have been scrutinized by different research groups [5–8]. The theoretical capacity exhibited by a graphite compound is 372 mAh/g based on $LiC_6$. In practice, this value is hardly achieved due to side reactions occurring during intercalation of lithium, especially in the first cycle. These unwanted reactions can be minimized by the correct choice of a liquid or a solid electrolyte. The use of a liquid electrolyte is not always compatible with carbonaceous materials, specially with graphite. However, during the electrochemical intercalation of lithium into graphite using propylene carbonate or methyl formate, graphite exfoliation and an electronic disconnection of the particles have been observed [9]. The destruction of the graphite structure is due to the co-insertion of the solvent molecules which are reduced, liberating a gas exfoliating the graphite sheets.

It has been shown that graphite exfoliation can be prevented by the use of a solid electrolyte.

The aim of this paper is to investigate different varieties of carbonaceous materials as the anodes for all solid batteries. In order to do so, various techniques such as galvanostatic cycling, electrochemical impedance spectroscopy, X-ray diffraction and electron energy loss spectroscopy (EELS) were used. Two types of carbon with different structures, a graphite and a coke were examined.

* Corresponding author.


*PII* S0378-7753(96)02430-5

## 2. Experimental

The different varieties of carbon used in this study came from different sources. The coke was from Conoco (USA), and the graphite materials, UF4, a natural one (grain size $\leq 20$ μm) and electrographite (a synthetic one, grain size $\leq 15$ μm) from Le Carbone Lorraine (France). Poly(ethylene oxide) (PEO) and the salt used, $LiN(CF_3SO_2)_2$ (denoted as LiTFSI), were from Aldrich (France) and 3M (USA), respectively. All the powders were used as received. The BET surface area was measured on a Micrometrics ASAP 2300 using a mixture of 70% of helium and 30% of nitrogen as the analysis gas, see Table 1.

### 2.1. X-ray diffraction measurements

X-ray characterizations were performed on as-received powders confined into Lindemann tubes. These measurements were obtained using a rotating anode Rigaku RU-200 B (Mo Kα radiation) coupled with a curve detector Inel CPS 120. The domain coherent size $L_c$ and $L_a$ were computed from the 004 and 110 lines of the graphite according, respectively, to Scherrer's equation [10], since diamond is used as a standard. The first ray of the latter appears at 9.916° and is used here as the instrumental function. The values are given in Table 2.

### 2.2. Electron energy loss spectroscopy

EELS measurements were conducted on a transmission electron microscope Philips CM20 operating at 200 kV with an unsaturated $LaB_6$ cathode. The EELS spectra were recorded in the diffraction mode coupling by means of a Gatan 666 parallel spectrometer. The cycled cells were dismounted in a glove box under pure argon atmosphere. The composite electrode after cycling was dissolved in acetonitrile and a suspension of thin graphite particles is obtained. A drop of this suspension is deposited onto a carbon grid. The grid is then mounted onto a cryogenic holder.

Table 1
BET surface area measurements

| Carbon | BET surface area ($m^2/g$) |
|---|---|
| Electrographite | 5.17 |
| UF4 | 15.15 |
| Coke | 3.555 |

Table 2
Measurements of $d_i$, $L_a$ and $L_c$

| | $d_i$ (pm) | $L_c$ (pm) | $L_a$ (pm) |
|---|---|---|---|
| Electrographite | 335 | 15000 | 38000 |
| Coke | 346 | | |

### 2.3. Preparation of different constituents of the cell

#### 2.3.1. Composite electrodes

45% (w/w) of the active material (carbon), 35% (w/w) of PEO (mol. wt. 900 000) and 15% (w/w) of the salt LiTFSI were dissolved in acetonitrile under magnetic stirring. An ultrasonic generator is then applied to this solution during 15 min enhancing the dispersion of the carbon particles.

The casting of the slurry is obtained by means of a K control coater KCC 302 from Erichsen. The copper substrate is set onto a grooved plate connected to a vacuum pump to keep it flat. The slurry was poured onto the substrate and by means of an adjustable micrometer scraper, the thickness of the coating can be monitored. The coatings were left to dry at room temperature. They were further dried at 110 °C under vacuum.

The thickness of the composite electrodes ranges from 40 to 50 μm. A lithium foil of 380 μm thickness from Chemetall (Germany) was used as the anode of the cell.

#### 2.3.2. Electrolyte

A molar ratio of PEO (mol. wt. 900 000) and LiTFSI of (O/Li = 21) was dissolved in $CH_3CN$. After complete dissolution, the viscous solution was cast onto a Teflon film using the K control coater and left untill complete evaporation of the solvent. The film obtained was further dried at 80 °C under vacuum. The electrolyte thickness was around 60 μm. It has to be pointed out that both the electrode and the electrolyte preparations were carried out in ambient air.

### 2.4. Fabrication of cells

The fabrication of cells was performed in a glove box under argon or dry air. The three constituents of the cell consisting of: (i) composite carbon cathode; (ii) solid electrolyte which also acts as a separator, and (iii) lithium anode pressed onto a nickel substrate were assembled as indicated in Fig. 1. The

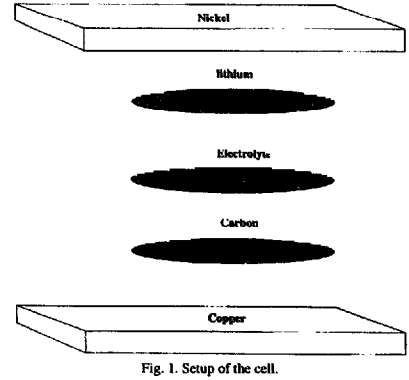


Fig. 1. Setup of the cell.

stacking of the three different layers were calendered under a pressure of 5 bar at 80 °C. The cell was then coated in a resin which kept it tight. The surface area of the active electrode was 7 $cm^2$.

### 2.5. Electrochemical measurements

The galvanostatic cycling measurements at 90 °C were done using a Macpile system. The cell was cycled between 3 and 0.01 V, with a current density of 0.028 $mA/cm^2$ at a temperature of 90 °C. The potential is given with respect to lithium. Charge and discharge of the cells refer, respectively, to the de-intercalation and intercalation of lithium into the carbonaceous materials.

The impedance measurement of the C/Li cells was measured between 10 mHz and 100 kHz using a Solartron frequency analyzer 1255 interfaced with a PAR 273 potentiostat/galvanostat controlled by an IBM PS/2 computer. The sinusoidal excitation voltage applied to the cells was 5 mV rms. The impedance data were collected at different stages, before cycling, after some hours of cycling and finally after cycling (failure of the cell) under an open-circuit condition. The impedance measurements in each of the above cases were repeated three times to ensure that the measured data were statistically significant.

## 3. Results and discussion

### 3.1. Galvanostatic cycling

Fig. 2 displays the curves at the first discharge (intercalation) and charge (de-intercalation) for different carbonaceous materials investigated. The open-circuit potential of the cell is 3.2 V. These results suggest strongly that the intercalation of lithium depends on the nature of carbon. Examination of these curves reveals an important loss in capacity, exhibiting a very low faradaic yield. This behaviour is in general encountered with carbonaceous materials specially in the first cycle. In addition to the electrochemical intercalation of lithium into carbonaceous materials, side reactions such as electrolyte reduction or formation of a passivation film on the carbon surface [6–8] can take place, thereby reducing the faradaic yield.

Table 3
Coulombic efficiencies after first and second cycles

| Carbonaceous material | $\eta_1$ (%) | $\eta_2$ (%) |
|---|---|---|
| Electrographite | 37.8 | 70 |
| UF4 | 43 | 77 |
| Coke | 40.73 | 71 |

With graphitized materials, such as natural or synthetic graphite, the typical charge/discharge curves displaying various plateaus at different potentials are characteristic of the different stages of lithium intercalation into graphite. In contrast, the intercalation of lithium into less-ordered materials, such as coke, does not give rise to any staged phase compound. The plateau at 0.8 V in the case of graphitized compound and at 1 V with coke can be attributed to electrolyte reduction.

Table 3 summarizes the faradaic yield measured after the first and second cycle, the faradaic yield being the ratio of the charge capacity to the discharge capacity.

It has to be pointed out that the initial capacity loss is much more important when cells operating with a liquid electrolyte. The wettability of the carbon electrode is relatively poor using a polymer electrolyte compared with a liquid electrolyte. This

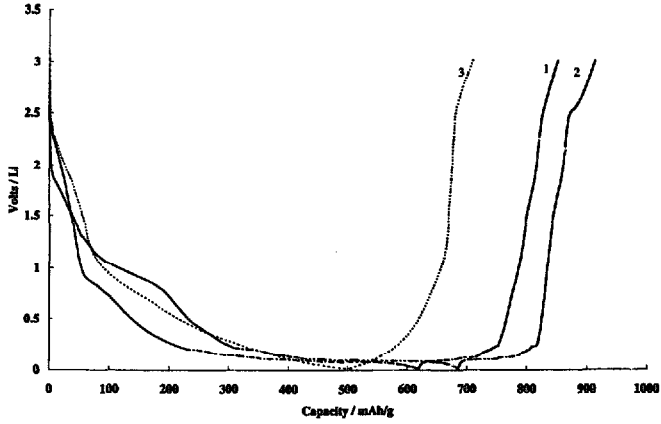


Fig. 2. Charge and discharge curves between 3 and 0.01 V with $i = 200$ μA at 90 °C: (1) electrographite, (2) UF4, and (3) coke.

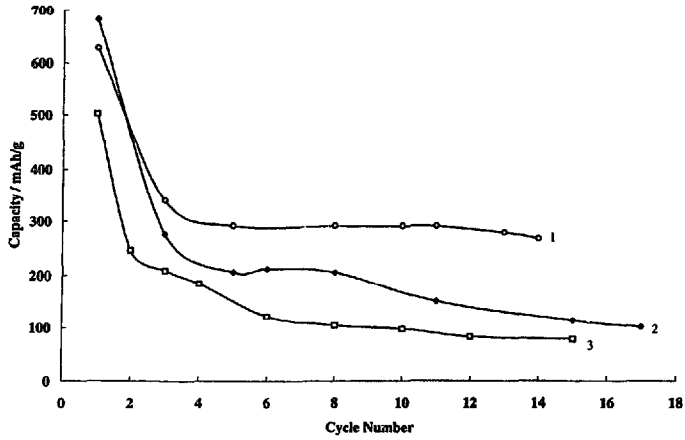


Fig. 3. Specific capacity vs. cycle number: (1) electrographite, (2) UF4, and (3) coke.

can affect the coulombic yield obtained in the first cycle. Moreover, it has been accepted that the intercalated lithium yielding $Li_\epsilon C_6$ remains imprisoned in the bulky carbon. This presumably will lower the faradaic yield.

Croce and Scrosati [11] put forward the existence of a passivation film at the Li/$(PEO)_8LiClO_4$ interface similar to the one reported in a liquid electrolyte. Consequently, during electrochemical intercalation of lithium into carbonaceous materials, a reaction between the intercalated lithium and the electrolyte can occur since the potential of $LiC_6$ is only 0.1 V with respect to lithium. This irreversible reaction should contribute to the low faradaic yield observed. After the first cycle, the reversibility improves yielding much higher coulombic efficiency.

Fig. 3 illustrates the curve of the specific discharge capacity versus cycle number. The most salient feature of the curve concerns electrographite which maintains its discharge capacity at 290 mAh/g after more than 15 cycles. In contrast, the capacity displayed by UF4 turns out to be 215 mAh/g for the first eight cycles, followed by a decline for the subsequent ones. Considering the different performances exhibited by the graphite materials, the nature (structure and morphology) of the material should play an important role.

After the first cycle, a drastic decline in capacity is observed for coke. The graphite material seems to be more interesting than the coke, as potent candidates in all solid lithium batteries. The specific discharge capacity exhibited by electrographite is much more attractive than the one obtained with pitch coke in a gelled electrolyte containing PEO, ethylene carbonate, propylene carbonate and $LiClO_4$ [12].

### 3.2. Influence of current density

The influence of the current density on the irreversible capacity has been undertaken. In this case, graphite was selected in view of their good discharge capacity compared with that of coke. The curves obtained are given in Figs. 4 and 5, respectively. In these two cases, a decrease in the irreversible capacity is obtained with an increase in current density. These results suggest the importance of monitoring the kinetics of lithium intercalation and de-intercalation in order to obtain maximum reversible capacity.

### 3.3. Influence of BET surface area

The irreversible capacity of the carbonaceous materials seems to be independent of the BET surface area as shown in Table 4. It is worth noting that the irreversible capacity loss measured with the coke in the first cycle is less than the one obtained with graphitized materials.

### 3.4. X-ray diffraction measurements

In an attempt to get insight into the structure and the capacity delivered by these compounds, X-ray diffraction measurements were performed. Fig. 6 depicts the spectra obtained on electrographite and coke. In the case of coke, narrow 00l reflections observed in the diffraction pattern of electrographite are substituted by broad bands characteristic of a material which displays practically no degree of organization along the $c$-axis direction. The high value of the reticular distance equals to 346 pm in the case of coke and the presence of a wide but a less intense hump provides evidence for this poor ordering. Moreover, the lack of in-plane ordering in coke is further supported by the absence of the 100 and 110 reflections recorded in the case of graphite, which are replaced by broad *hk* bands. The low capacity exhibited by coke cannot be assigned to the different staging mechanisms found in graphite but could rather be attributed to impurities

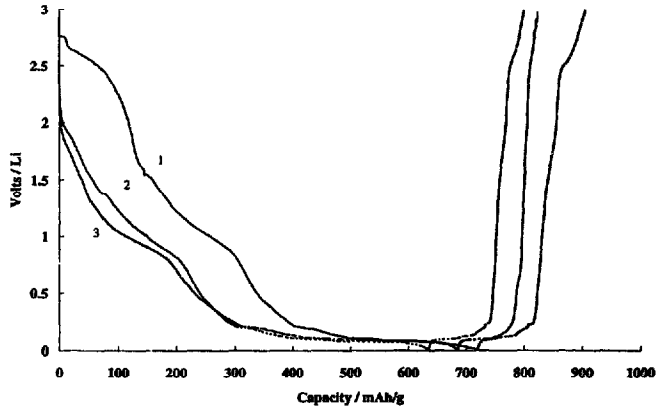


Fig. 4. Charge and discharge curves for UF4 between 3 and 0.01 V with different $i$ values at 90 °C: (1) 0.03 mA, (2) 0.09 mA, and (3) 0.2 mA.

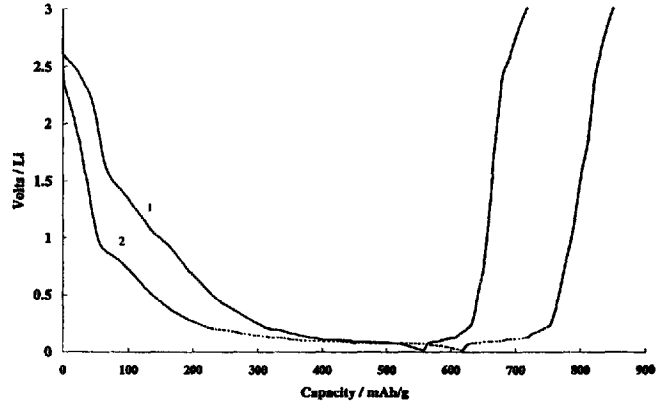


Fig. 5. Charge and discharge curves for electrographite between 3 and 0.01 V with different $i$ values: (1) 0.04 mA, and (2) 0.2 mA.

mainly of acceptor types, which decrease the Fermi level of graphite, thus raising the intercalation potential as shown in Fig. 2 [13]. It has to be emphasized that in the case of graphite, lithium intercalation occurs mainly at a potential below 0.25 V; results which are consistent with those reported in Refs. [14,15].

Table 4
Measurements of BET surface area and % of irreversible capacity

| Carbonaceous material | Surface BET ($m^2/g$) | % Irreversible capacity |
|---|---|---|
| Electrographite | 5.17 | 61.2 |
| UF4 | 15.154 | 67.41 |
| Coke | 3.555 | 40.8 |

### 3.5. Electrochemical impedance spectroscopy

The measurements of spectra before and after cycling were carried out on different cells. This non-destructive technique yields the possibility to examine the different interfaces during cycling. Moreover, it has been used successfully to assess the degradation process in other battery systems [15–18].

The interpretation of our impedance spectra relies upon a simplified equivalent circuit of Randle's type developed for intercalation compounds [15].

Fig. 7 illustrates the impedance spectra obtained on symmetrical cells composed of Li/$(PEO)_{21}$ LiTFSI/Li before and after 200 h of cycling, the current density being 0.1 mA/$cm^2$. Two intercepts on the real axis can be identified. The

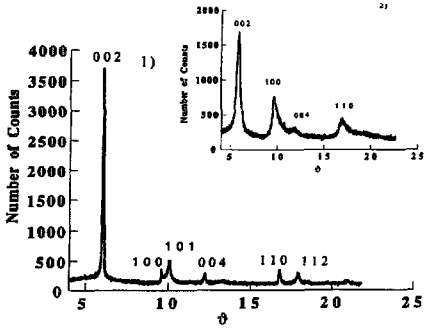


Fig. 6. X-ray spectra: (1) electrographite, and (2) coke.

first one, at high frequency, may be attributed to the electrolyte resistance, and the second one, at low frequency, to the charge-transfer resistance [19]. The line inclined at 45° on the real axis can be ascribed to the diffusion of $Li^+$. After 200 h of cycling, a slight increase in diameter of the semi-circle is observed. However, the height of the diameter of the semi-circle remains unchanged.

Impedance spectra were also recorded on cells of different types of carbon before and after cycling (failure of the cell) under an open-circuit condition. Figs. 8 and 9 showed the spectra obtained on different graphite, UF4 and electrographite, respectively.

In the case of UF4, an increase in diameter and height of the semi-circle is observed. However, for electrographite whose discharge capacity reached a value of 290 mAh/g, the variation of the impedance spectra is less significant. Comparison of the spectra indicates an increase in the charge-transfer resistance.

Analysis of the spectra of $C/(PEO)_{21}LiTFSI/Li$ with $Li/(PEO)_{21}LiTFSI/Li$ reveals an intensive modification of the $C/(PEO)_{21}LiTFSI$ interface. The impedance of the cell $UF4/(PEO)_{21}LiTFSI/Li$ increases by a factor of 16. Assuming that the equivalent circuit holds in our cases, we found that the electrolyte conductivity was decreased by a factor of 75.

For the natural graphite UF4, it was found that a decrease in discharge capacity was associated with an increase in impedance of the cell. Such an increase can be due to different factors such as changes occurring at the cathode interface, at the anode interface or in the bulk electrolyte. Of course, all these changes are detrimental for achieving extended cycleability. At potentials lower than 0.1 V, reaction between the superficial lithium and the electrolyte can be expected. If the superficial lithium reacted with the conducting salt, the electrolyte would be depleted of the salt resulting in a decrease in conductivity. Similarly, a reaction between PEO and the superficial lithium would cause the salt concentration to be increased to such an extent that the conductivity of the electrolyte would be drastically reduced. These reactions are more likely to occur on natural graphite than on the synthetic one, since the former has a greater surface area and is more sensitive to the electrolyte, as evidenced by the impedance measurements. The drastic decrease in conductivity could contribute mostly to the increase in impedance of the cell.

Inspection of the graphite materials on a transmission electron microscope reveals the existence of a layer. Analysis by

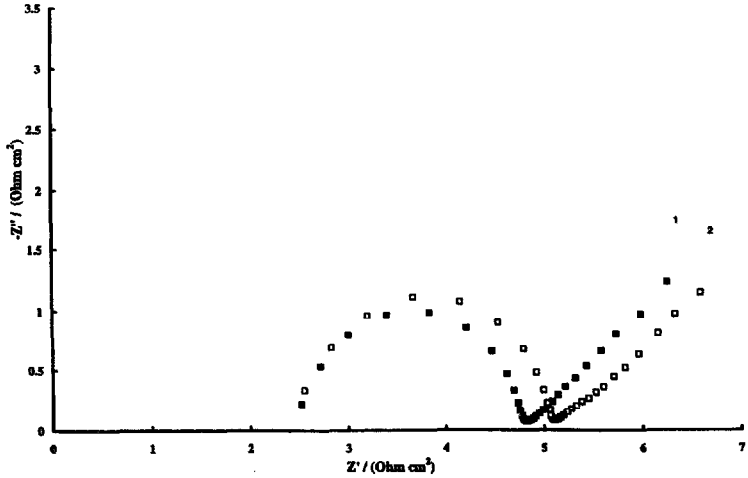


Fig. 7. Nyquist diagram of a symmetrical cell Li/(PEO)LiTFSI/Li at 90 °C: (1) before cycling, and (2) after cycling; $i = 0.7$ mA.

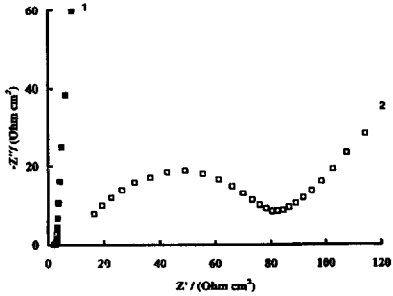


Fig. 8. Nyquist diagram of a cell Li/(PEO)LiTFSI/UF4 at 90 °C: (1) before cycling, and (2) after cycling; $i = 0.2$ mA.

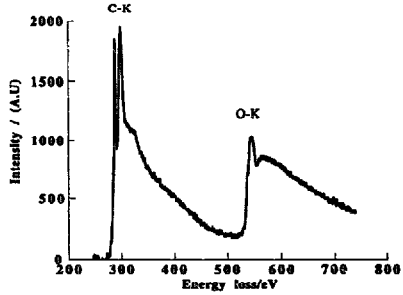


Fig. 10. EELS spectrum of carbonates found on graphite

EELS indicates that the layer is composed mainly of carbon and oxygen. To fully characterize this layer, we examined the fine structure of the threshold level of the carbon. The analysed carbon yields the presence of two peaks, one located at 288 eV and the other one at 299 eV, which are characteristic of the following transitions: $1s \rightarrow \pi^*$ of the C=O bond and $1s \rightarrow \sigma^*$ of the C–O bond (Fig. 10), respectively. Furthermore, quantitative analysis of the C/O ratio yielding a value of 2.8 suggests that the layer consists of carbonates. A deeper analysis in the low energy loss zone displays the presence of lithium. To corroborate this finding, we examined a commercial lithium carbonate sample. Its EELS spectra and the C/O ratio were identical to the one found on UF4. We did not understand the exact mechanism of the formation of carbonates. It could be due to a complicated reaction involving the reduction of the electrolyte by the superficial lithium. In the case of coke, the variation of the total impedance before and after cycling is less pronounced. These results suggest that electrolyte degradation takes place mainly during the first cycle while a progressive degradation is observed in the case of graphite compounds.

## 4. Conclusions

The electrochemical intercalation of lithium was conducted on a different carbonaceous materials. The performances exhibited by the graphite compounds are greater than those exhibited by coke.

Among the graphite materials investigated, a specific discharge capacity of 290 mAh/g after more than 15 cycles is obtained with electrographite whose BET surface area is three times less than the UF4. For a given graphite, the initial irreversible capacity loss during the first cycle seems to be inversely proportional to the current density. While the variation of the impedance spectra of the synthetic graphite before and after cycling is less significant, a sharp increase is found in the case of the natural one, resulting in a drastic decrease in discharge capacity. This jump is probably caused

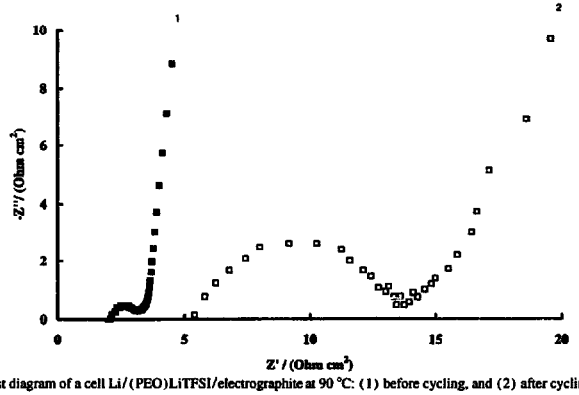


Fig. 9. Nyquist diagram of a cell Li/(PEO)LiTFSI/electrographite at 90 °C: (1) before cycling, and (2) after cycling; $i = 0.2$ mA.

by an irreversible reduction of the electrolyte which is more likely to occur on the natural graphite with a greater BET surface area.

The irreversible capacity measured on coke is less than the one found on graphite materials. Moreover, electrolyte degradation seems to be less severe on this material.

## Acknowledgements

One of the authors (F.C.) would like to thank D. Livigni for his technical assistance and Dr G. Medjahdi for performing the X-ray diffraction measurements.

## References

[1] T. Nagaura, *4th Int. Rechargeable Battery Seminar, Deerfield Beach, FL, USA, 1990.*
[2] A.N. Dey, *J. Electrochem. Soc., 118* (1971) 1547.
[3] I. Epelboin, M. Froment, M. Garreau, J. Thevenin and D. Warin, *J. Electrochem. Soc., 127* (1980) 2100.
[4] J.R. Van Beek and P.J. Rommers, in J. Thompson (ed.), *Power Sources 7*, Academic Press, London, 1979, p. 595.
[5] R. Yazami and D. Guérard, *J. Power Sources, 43/44* (1993) 39.
[6] T. Ohzuku, Y. Iwakoshi and K. Sawai, *J. Electrochem. Soc., 140* (1993) 2490.
[7] R. Fong, V. Von Sacken and J.R. Dahn, *J. Electrochem. Soc., 137* (1990) 2009.
[8] R. Kanno, Y. Kawamoto, Y. Takeda, O. Yamamoto and M. Inagaki, *J. Electrochem. Soc., 139* (1992) 3397.
[9] D. Aurbach, Y. Ein-Eli, O. Chusid, Y. Carmeli, M. Babai and H. Yamin, *J. Electrochem. Soc., 141* (1994) 603.
[10] A. Guinier, *Théorie et Technique de la Radiocristallographie*, Dunod, Paris, 2nd. edn., 1956, p. 498.
[11] F. Croce and B. Scrosati, *J. Power Sources, 43/44* (1993) 9.
[12] C.E. Newnham, S. Rinne and N. Schoeley, *J. Power Sources, 54* (1995) 516–518.
[13] J. Maire and J. Mering, *Chem. Phys. Carbon, 6* (1970) 125.
[14] J.R. Dahn, R. Fong and M.J. Spoon, *Phys. Rev. B, 42* (1990) 6424.
[15] J.R. Dahn, U. Von Sacken, M.W. Juzkow and H. Al-Janaby, *J. Electrochem. Soc., 138* (1991) 2207.
[16] C. Ho, I.D. Raistrick and R.A. Huggins, *J. Electrochem. Soc., 127* (1980) 343.
[17] J.G. Thevenin and R.H. Muller, *J. Electrochem. Soc., 134* (1987) 273.
[18] A.J. Hills, N.A. Hampson and M. Hayes, *J. Electrochem. Soc., 209* (1986) 351.
[19] G.E. Lagos, N. Bonanos and B.C.H. Steele, *Electrochim. Acta, 28* (1983) 1581.